Polycystin-2, the protein mutated in autosomal dominant polycystic kidney disease (ADPKD), is a Ca^{2+}-permeable nonselective cation channel

Silvia González-Perrett*†, Keetae Kim†‡, Cristina Ibarra*§, Alicia E. Damiano*§, Elsa Zotta§, Marisa Batelli*, Peter C. Harris¶, Ignacio L. Reisin*‖, M. Amin Arnaout‡, and Horacio F. Cantiello*‡***

*Laboratorio de Canales Iónicos, Departamento de Fisicoquímica y Química Analítica, Facultad de Farmacia y Bioquímica, Buenos Aires, Argentina 1113; ‡Renal Unit, Massachusetts General Hospital East, Charlestown, MA, 02129 and Department of Medicine, Harvard Medical School, Boston, MA 02115; §Departamento de Fisiología, Facultad de Medicina, Buenos Aires, Argentina 1121; and ¶Department of Nephrology, Mayo Clinic, Rochester, MN 55905

Edited by Maurice B. Burg, National Institutes of Health, Bethesda, MD, and approved November 13, 2000 (received for review September 22, 2000)

Defects in polycystin-2, a ubiquitous transmembrane glycoprotein of unknown function, is a major cause of autosomal dominant polycystic kidney disease (ADPKD), whose manifestation entails the development of fluid-filled cysts in target organs. Here, we demonstrate that polycystin-2 is present in term human syncytiotrophoblast, where it behaves as a nonselective cation channel. Lipid bilayer reconstitution of polycystin-2-positive human syncytiotrophoblast apical membranes displayed a nonselective cation channel with multiple subconductance states, and a high perm-selectivity to Ca^{2+}. This channel was inhibited by anti-polycystin-2 antibody, Ca^{2+}, La^{3+}, Gd^{3+}, and the diuretic amiloride. Channel function by polycystin-2 was confirmed by patch-clamping experiments of polycystin-2 heterologously infected Sf9 insect cells. Further, purified insect cell-derived recombinant polycystin-2 and *in vitro* translated human polycystin-2 had similar ion channel activity. The polycystin-2 channel may be associated with fluid accumulation and/or ion transport regulation in target epithelia, including placenta. Dysregulation of this channel provides a mechanism for the onset and progression of ADPKD.

Autosomal dominant polycystic kidney disease (ADPKD) is the most common monogenic disease in humans, with a frequency ranging from 1:400 to 1:1000 (1, 2). The cardinal feature of ADPKD is the formation of renal cysts (3) that lead, over time, to progressive destruction of normal tissue and end stage kidney failure. ADPKD is caused by mutations in either one of two genes, *PKD1* or *PKD2. PKD1* encodes polycystin-1, an 11-membrane-spanner glycoprotein with a large extracellular region composed of a unique compilation of potential adhesion and protein–protein interaction domains (4, 5). *PKD2* encodes polycystin-2, a 6-membrane spanner, with cytoplasmic N- and C-termini, and with homology to voltage-activated calcium and sodium channels (6). The function of polycystins-1 or -2 is unknown (7, 8). However, the two proteins have been shown to interact through their cytoplasmic tails, leading to the suggestion that polycystin-1 may play a regulatory role as a ligand that binds (7) and regulates the putative channel activity of polycystin-2 (2, 7). This hypothesis, however, awaits experimental proof.

The microvillous structure of the syncytiotrophoblast (hST) is the most apical membrane of the human placenta, which provides a perm-selective barrier for electrolyte transfer between mother and fetus (9). Little is known about the transport mechanisms responsible for cation movement in hST. Recently, polycystin-2 was detected in human placenta (10). Here, we used lipid bilayer reconstitution of hST apical membranes to identify a nonselective cation channel, inhibitable by a monospecific antibody to polycystin-2. *PKD2*-containing baculovirus-infected Sf9 insect cells expressing recombinant human polycystin-2 displayed a similar channel profile. In addition, flag-tagged human recombinant polycystin-2, purified from Sf9 insect cells, and the *in vitro* translated human polycystin-2 exhibited similar ion channel properties. To our knowledge, there have been no other findings that establish the channel nature of polycystin-2, thus directly linking the defect in ADPKD to abnormal ion transport.

Materials and Methods

Human Placenta Membrane Preparation. hST membrane vesicles were obtained from term human placenta as described (11), following institutional consent guidelines. Apical membrane enrichment was ≈26-fold from initial homogenate. Membranes were suspended in a buffer solution containing 10 mM Hepes-KOH (pH 7.4), 250 mM sucrose, and 20 mM KCl.

Ion Channel Reconstitution. Membrane vesicles were reconstituted onto planar lipid bilayers as previously described (11). Briefly, lipid bilayers were formed with a mixture of synthetic 1-palmitoyl-2-oleoyl-choline and ethanolamine (25 mg/ml, Avanti Polar Lipids) in *n*-decane. Electrical signals were filtered (700 Hz) with an eight-pole Bessel filter (Frequency Devices, Haverill, MA), digitized with a pulse code modulator, and stored in videotapes.

Calculation of Single Channel Conductances, Subconductance States, and Perm-Selectivity Ratios. Currents were analyzed with PCLAMP (Version 5.5.1), and further filtered for display purposes. Single channel conductances were calculated by fitting experimental data to either a straight line or the Goldman-Hodgkin-Katz (GHK) equation (12). Ionic perm-selectivity ratios were calculated with a modified version of the GHK (12), where the P_{Ca}/P_K ratio was fitted to the experimental data in the presence of K^+ and Ca^{2+}, with $(1 + \exp(-FV/RT)\{K_c - K_t[\exp(-FV/RT)]\})/(4\{[Ca_t \exp(-2FV/RT)] - Ca_c\})$, where c = cis chamber, t = trans chamber, V = reversal potential, F = Faraday constant, R = the gas constant, T = absolute temperature, and Ca^{2+} and K^+ are the mean activities for either cation, respectively. A similar approach was conducted for other mono-divalent cation interactions. Data were expressed as the mean ± SEM.

Solutions. Both sides of the lipid bilayer contained 10–15 μM Ca^{2+}, 10 mM Mops-KOH, and 10 mM Mes-KOH (pH 7.4). The

This paper was submitted directly (Track II) to the PNAS office.

Abbreviations: ADPKD, autosomal dominant polycystic kidney disease; hST, human syncytiotrophoblast.

See commentary on page 790.

†S.G.-P. and K.K. contributed equally to this work.

**To whom reprint requests should be addressed at: Renal Unit, Massachusetts General Hospital, 149 13th Street, Charlestown, MA 02129. E-mail: cantiello@helix.mgh.harvard.edu or arnaout@receptor.mgh.harvard.edu.

‖Deceased November 8, 1998.

The publication costs of this article were defrayed in part by page charge payment. This article must therefore be hereby marked "*advertisement*" in accordance with 18 U.S.C. §1734 solely to indicate this fact.

Article published online before print: *Proc. Natl. Acad. Sci. USA*, 10.1073/pnas.021456598. Article and publication date are at www.pnas.org/cgi/doi/10.1073/pnas.021456598

final K^+ concentration was approximately 15 mM. KCl (135 mM) was also added (cis). Whenever indicated, the trans compartment contained either KCl, NaCl, or $CaCl_2$, to final concentrations of 150, 135, and 90 mM, respectively.

Other Reagents. Chemicals were purchased from Sigma unless otherwise stated. Amiloride (10 mM) was kept in DMSO. $LaCl_3$ and $GdCl_3$ stock solutions (100 mM) were prepared in distilled water. The anti-polycystin-2 antibody was directed against a bacterial fusion protein containing the C-terminal 258 aa of polycystin-2 (10). An anti-flag antibody (M2 mAb, Eastman Kodak) against the sequence DYKDDDDK was used to purify and detect the flag-tagged polycystin-2.

Total RNA Isolation. Total RNA was isolated from hST by using the SV RNA Isolation System (Promega), quantified by absorbance (260 nm) and stored at −80°C.

Reverse Transcription (RT)-PCR Assay. RT-PCR of hST total RNA (2 μg) was conducted for 60 min at 42°C, using Moloney murine leukemia virus reverse transcriptase (Promega), oligo$(dT)^{15}$ primers, and dNTP (400 μM each). PCR (thirty 1-min cycles at 94°C, 58°C, and 72°C, and final extension at 72°C, 10 min) was carried out with two specific primers from the C termini of human *PKD2* (5′-TCC GAT GAT GCA GCT TCC CAG AT-3′ and 5′-ATT GCC CCA TTT TCC TTC ACA CTC-3′) and *PKDL* sequences (13). Inactivated RT was included to detect DNA contamination. RT-PCR products were separated by agarose gel electrophoresis (1.8%).

Polycystin-2 Expression in Sf9 Cells. The flag-tagged *PKD2* complete coding sequence was obtained by assembly of the coding region clones K1-1 (6) and CTM4B3-3 (Genome Systems, St. Louis) into the baculovirus vector pVL1393. The flag was added in-frame at the 3′ end. The DNA construct (1 mg/ml in distilled water) was used to transfect Sf9 insect cells (5×10^6) with cationic liposomes (Invitrogen) and 0.5 mg of a deleted version of baculovirus DNA (PharMingen). Recombinant baculovirus containing *PKD2*-flag-tagged cDNA was titrated by plaque assay, and expression of polycystin-2 in Sf9 cells was confirmed by Western blot analysis with the anti-flag M2 antibody.

The *PKD2*-baculovirus infected cells (72 h) were harvested and washed by centrifugation (2,000 × *g*) in PBS. Cells were lysed in 10 mM Tris (pH 7.5), 130 mM NaCl, and 1% Triton-X100, with the proteinase inhibitors PMSF (1 mM, Boehringer Mannheim), leupeptin (10 μg/ml, Sigma), and aprotenin (1 μg/ml, Sigma). The cell lysate was cleared by centrifugation (40,000 × *g*, 30 min, 4°C) and applied to an anti-flag M2 agarose gel preequilibrated with TBS (50 mM Tris/150 mM NaCl, pH 7.4). Flag-tagged polycystin-2 was eluted with 100 mM glycine (0.5 ml, pH 3.5) into vials containing 2 μl of 1 M Tris (pH 8.0) and dialyzed against TBS (3×, 4-h intervals, 4°C). Approximately 0.5 μg of the purified nondegraded protein was obtained from 10^7 infected Sf9 cells.

***In Vitro* Translation of the *PKD2* Gene Product.** A 3.2-kb *Xba*I-*Pst*I fragment encoding the flag-tagged polycystin-2 from pVL1393-*PKD2* was transferred to *Xba*I-*Nsi*I site of pGEM-7zf(+) to generate the plasmid pGEM-PKD2. This cDNA was transcribed and translated *in vitro* with the TnT-T7 coupled reticulocyte lysate system (Promega) in the presence or absence of microsomal membranes. Plasmid DNA (1 μg) and the *in vitro* reaction mixture (50 μl), including L-[^{35}S]methionine (Amersham), were incubated for 90 min at 30°C. *In vitro* translated ^{35}S-labeled polycystin-2 and luciferase (as control) were analyzed by SDS/PAGE and autoradiography.

Western Blot and Immunocytochemical Analysis. Membranes of hST were dissolved in SDS loading buffer, heated (2 min, 100°C), and resolved on 7.5% polyacrylamide gels. Nitrocellulose membranes with electrotransferred proteins were blocked with BSA in PBS (1% wt/vol), and incubated with anti-polycystin-2 antibody (1:1000, 60 min). The secondary antibody was a rat anti-rabbit, peroxidase-conjugated IgG (1:2,500). Samples were visualized with the ECL plus detection system (Amersham Pharmacia). For immunocytochemistry, hST was fixed in ice-cold paraformaldehyde (4%, PBS), dehydrated, and embedded in cytoparaffin. Consecutive, thin sections (4–5 μm) were cut, permeabilized with Triton X-100 (0.1%), washed extensively with PBS, and incubated overnight (4°C) with anti-polycystin-2 antibody (1:400). Samples were examined by optical microscopy after rinsing and incubation (2 h, room temperature) with anti-rabbit Cy3 (1:200).

Results

Characterization of an hST Cation Channel. Membrane vesicles of term hST were reconstituted in the presence of a KCl chemical gradient, where a cation-selective channel was observed in most experiments (481/533) with spontaneous channel activity (Fig. 1*a*). Although most membranes contained numerous channels, a main single channel conductance of 177 ± 5.0 pS ($n = 10$) was obtained from single channel tracings (Fig. 1*b*). Single channel currents frequently displayed subconductance states (Fig. 1*c*), which averaged 32.5 ± 1.92 pS ($n = 3$), 65.3 ± 2.78 pS ($n = 8$), 91.1 ± 2.66 pS ($n = 5$), and 119 ± 6.05 pS ($n = 5$). The Cl^-/K^+ perm-selectivity ratio was lower than 0.02. The main single channel conductance in symmetrical KCl (150 mM, Fig. 1*d*) was 134 ± 7.3 pS ($n = 6$) (Fig. 1*e*). Single channel currents were also highly linear after equimolar replacement of trans K^+ with Na^+ (Fig. 1*f*), indicating a Na^+/K^+ perm-selectivity ratio of 1.1. Thus, this channel species, although cation-selective, was largely permeable to both cations. The channel was permeable to Cs^+ and Ba^{2+} (data not shown), and channel activity was also observed in a K^+ chemical gradient after addition of Ca^{2+} (90 mM) to the trans chamber (Fig. 1*g*). The reversal potential, 10 mV (Fig. 1*e*), indicated that the nonselective cation channel of hST was more permeable to Ca^{2+} than to monovalent cations, with a Ca^{2+}/K^+ perm-selectivity ratio of 1.3. However, Ca^{2+} movement also inhibited K^+ channel activity in hST (Fig. 1*h*). The hST nonselective cation channel displayed an evident voltage dependence of the open probability, particularly at positive potentials (Fig. 1*a*). The channel was inhibited by addition of La^{3+} (Fig. 2*a*), Gd^{3+}, and by a reduction in pH_{cis} (data not shown). The nonselective cation channel of hST was also blocked by amiloride (Fig. 2*b*), with an inhibitory constant of 27.0 ± 8.1 μM ($n = 15$). Amiloride is a known inhibitor of various Na^+-permeable epithelial cation channels (14–16).

The hST Cation Channel Is Identical with Polycystin-2. The nonselective cation channel of hST had similar functional features to those ascribed to polycystin-L (17). Polycystin-L shares sequence homology with polycystin-2 (6, 13, 18), a protein of unknown function that is defective in 10–15% of all patients with ADPKD (8). Addition of anti-polycystin-2 antibody [1:10 dilution (10)], but not preimmune serum (data not shown), reduced hST K^+ channel activity ($n = 3$, Fig. 2*c*). These data suggest a possible link between the hST nonselective cation channel and polycystin-2. The presence of polycystin-2 in hST was confirmed by RT-PCR, where an expected band of ≈570 bp was found in hST mRNA using specific primers for *PKD2* but not for *PKDL* (Fig. 2*d*). Western blot (Fig. 2*e*) and immunocytochemical analyses (Fig. 2 *f* and *g*) also revealed the presence of polycystin-2 in the apical membrane of hST microvilli (Fig. 2*g*).

The functional role of polycystin-2 as an ion channel was confirmed by patch-clamping and reconstitution experiments of

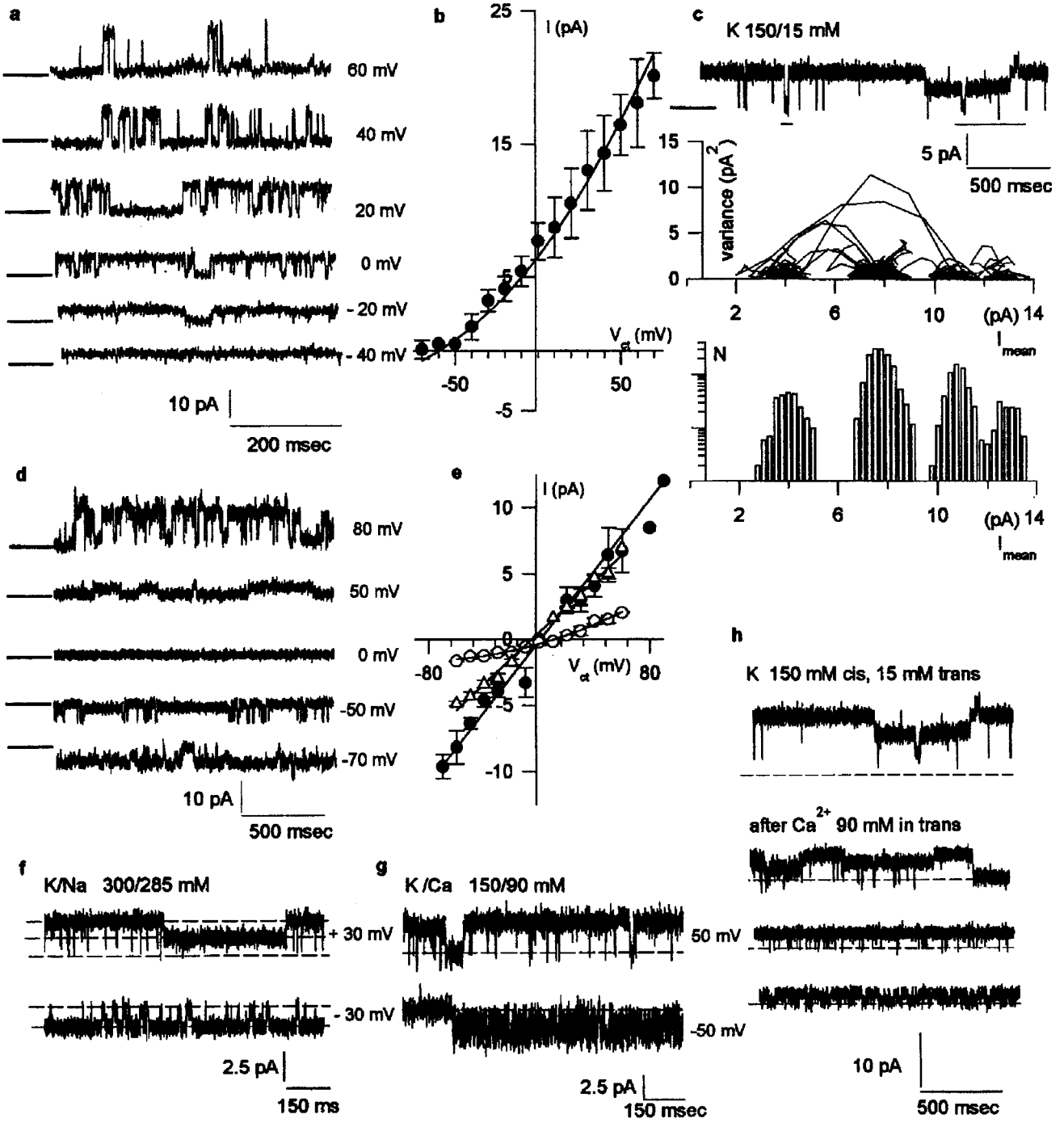

Fig. 1. Nonselective cation channel of hST. (*a*) Single channel currents in asymmetrical KCl (150/15 mM). Tracings were filtered at 50 Hz to show the unitary conductance in the absence of subconductance states. Holding potentials are indicated on the right. (*b*) Current-to-voltage (I/V) relationship in asymmetrical KCl ($n = 10$) was fitted with the Goldman-Hodgkin-Katz (GHK) equation (solid line). (*c*) Multiple conductance substates (*Top*) were identified as mean vs. variance plots (*Middle*), and low variance histograms (*Bottom*). (*d*) Single channel currents in symmetrical KCl (150 mM). (*e*) I/V relationships in KCl (filled circles, $n = 6$), Na^+/K^+ (open triangles, $n = 6$) and K^+/Ca^{2+} (open circles, $n = 3$). (*f*) Single channel currents in K^+/Na^+ ($n = 6$), and K^+/Ca^{2+} (*g*, $n = 3$). (*h*) Inhibition of (cis) K^+ currents by addition of Ca^{2+} in trans ($n = 3$).

the purified protein. Flag-tagged polycystin-2 was expressed by baculoviral infection of Sf9 insect cells (19, 20) (Fig. 3*a*). Functional expression of flag-tagged polycystin-2 in the plasma membrane of infected Sf9 cells was first determined by cell-attached and excised inside-out patch-clamping experiments. Mono- and divalent cation-permeable ion channels (Fig. 3) were observed under cell-attached (9/15, Fig. 3*b*) and excised (35/35, Fig. 3*c*) conditions. Single channel currents in asymmetrical Cs^+/Na^+ (150 mM) were observed with average conductances of 16.0 ± 0.14 pS ($n = 8$), 32.0 ± 0.32 pS ($n = 10$), and 78 ± 0.87 pS ($n = 7$) (Fig. 3*f*), suggesting multiple channel levels, and clustering, because not all multiples were observed. Less frequent conductance levels were also found of 206 ± 31 pS ($n = 2$), 264 ± 14.0 pS ($n = 2$), and 528 ± 27 pS ($n = 3$), further

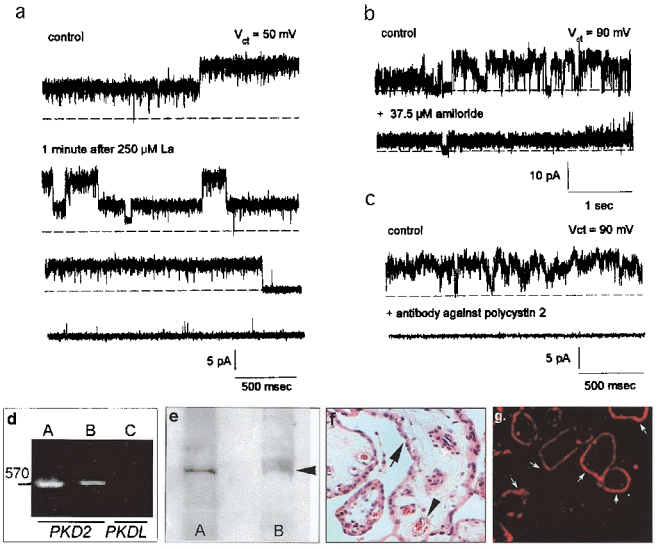

Fig. 2. Inhibition of cation channels, and expression of polycystin-2 in hST. Single channel K^+ currents were inhibited by La^{3+} (*a*, $n = 3$), by amiloride (*b*, $n = 5$), and anti-polycystin-2 antibody (1:10 dilution, $n = 3$) added to the cis side of the chamber (*c*). (*d*) RT-PCR with *PKD2* (≈570 bp, lane B) but not *PKDL* primers (lane C). Positive control was mouse kidney (lane A). (*e*) Western blot analysis of ≈110-kDa protein corresponding to polycystin-2 (lane B, arrow). Lane A indicates fetal rat kidney as positive control. (*f*) Hematoxylin & eosin staining of hST, indicating apical syncytial epithelial cells (arrows), and vessels (arrow heads) (×180). (*g*) Polycystin-2 immunolocalized to the apical membrane (arrows).

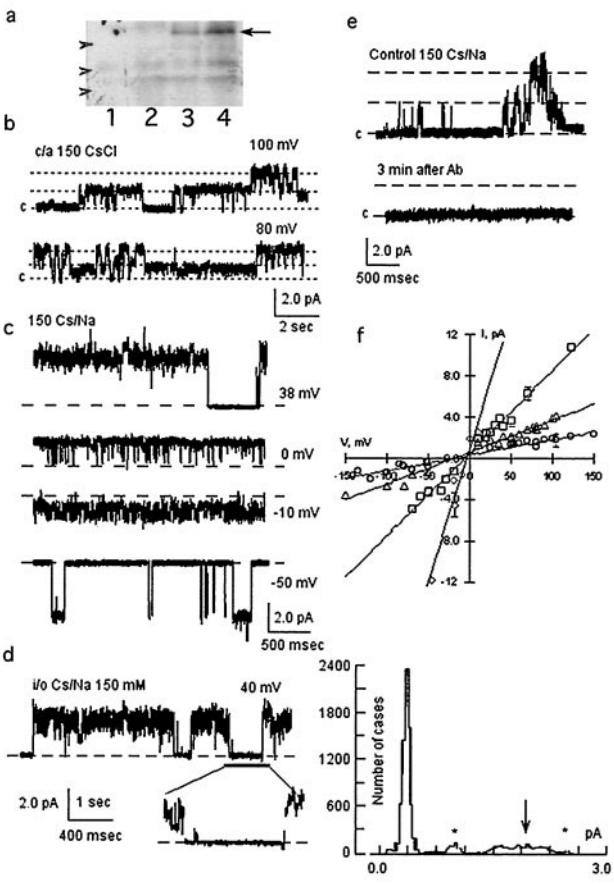

Fig. 3. Expression of polycystin-2 in Sf9 insect cells. (*a*) Western blots of Sf9 cell extracts infected either with baculovirus lacking the polycystin-2 cDNA insert (lanes 1 and 2) or containing (lanes 3 and 4) polycystin-2 cDNA viral inserts from two independent clones. The position of recombinant polycystin-2 (≈110 kDa) is indicated by the arrow. Arrowheads indicate the position of GIBCO/BRL molecular weight markers (from top to bottom 97.4 kDa, 68 kDa, and 43 kDa, respectively). Extracts from $\approx 10^6$ cells are shown in each lane. (*b*) Single channel currents of cell-attached (c/a) patches of infected Sf9 cells. Channel activity was observed in the presence of CsCl (150 mM) in the pipette. Data are representative of nine experiments. (*c*) Single channel currents of excised inside-out patches. Data in Cs^+/Na^+ (150 mM) are representative of 35 experiments. (*d Left*) Single channel currents of infected Sf9 cells showed subconductance states (expanded tracing at the bottom), and further indicated by all-point histogram (*Right*). Subconductance states are indicated by asterisks, and main conductance by the arrow. (*e*) Polycystin-2-mediated single K^+ currents were blocked by anti-flag antibody ($n = 3$). (*f*) Current-to-voltage relationships of most frequent single channel conductances, with average conductances of 16 pS (open circles, $n = 8$), 32 pS (open triangles, $n = 10$), 78 pS (open squares, $n = 7$), and 264 pS (open diamonds, $n = 3$).

suggesting channel clustering of various conductance levels. Channel substates were confirmed at different holding potentials (Fig. 3*d*). No shift in reversal potential was observed by replacement of Cl^- with either gluconate or aspartate (data not shown), but a 10.7-mV shift in reversal potential (−12.7 mV vs. −2.08 mV) was observed by replacement of Na^+ (150 mM) for Ba^{2+} (70 mM), suggesting a Cs^+/Ba^{2+} perm-selectivity ratio of 0.65. Thus, the channel was more permeable to divalent than monovalent cations. No cation-selective channel activity was observed in naive Sf9 cells ($n = 15$, data not shown), as previously reported (21). Polycystin-2 channel activity could be blocked by anti-flag antibodies (Fig. 3*e*). Two other strategies were also followed to directly assess polycystin-2 channel function. First, flag-tagged polycystin-2 was purified from polycystin-2-expressing Sf9 cells with anti-flag antibody-coupled agarose beads. A second strategy consisted of the *in vitro* transcription/translation of the flag-tagged *PKD2* gene product. Affinity-purified polycystin-2 displayed cation-selective ion channel activity (62/70, Fig. 4*a*), the remaining also showing anion permeability (data not shown). Channel function was observed in asymmetrical K^+ (150/15 mM, Fig. 4*b Upper*) and symmetrical K^+ (Fig. 4*b Lower*). A main single channel conductance of 138 ± 6.24 pS ($n = 18$) was obtained, although various subconductance levels (Fig. 4*b*), identical to those observed in the hST nonselective cation channel (Fig. 4*e*), were also frequently observed. Purified polycystin-2 was permeable to Na^+, Cs^+, Ba^{2+}, and Ca^{2+}. However, Ca^{2+} was also an inhibitor of polycystin-2 channel function. Amiloride (Fig. 4*c*) also inhibited channel function, with an inhibitory constant of 79.4 ± 23.3 μM ($n = 8$), not statistically different from that of hST. The anti-polycystin-2 antibody (Fig. 4*d*) also inhibited polycystin-2 channel activity as observed for the hST cation-selective ion channel. Similarly, the *in vitro* translation *PKD2* product (Fig. 5*a*) displayed cation-selective ion channel activity (24/24, Fig. 5*b*). Single channel currents, with main conductances of 25.5 ± 2.7 pS ($n = 6$), 73.4 ± 3.70 pS ($n = 6$), and 138 ± 9.7 pS ($n = 3$) (Fig. 5 *b* and *d*), were observed with the presence of frequent subconductance states (Figs. 5 *c–e*). *In vitro* translated polycystin-2 was also inhibited by amiloride (data not shown). Negative (control) experiments were also conducted on both patches and membranes of uninfected Sf9 cells and *in vitro* transcribed/translated unrelated products (luciferase), which under no conditions displayed any channel activity.

Discussion

The data presented in this report establish that the *PKD2* gene product, polycystin-2, is present in human term syncytiotrophoblast, where it behaves as a nonselective cation channel with multiple substates and a high permeability to Ca^{2+}. Several features of polycystin-2 resembled those recently observed for

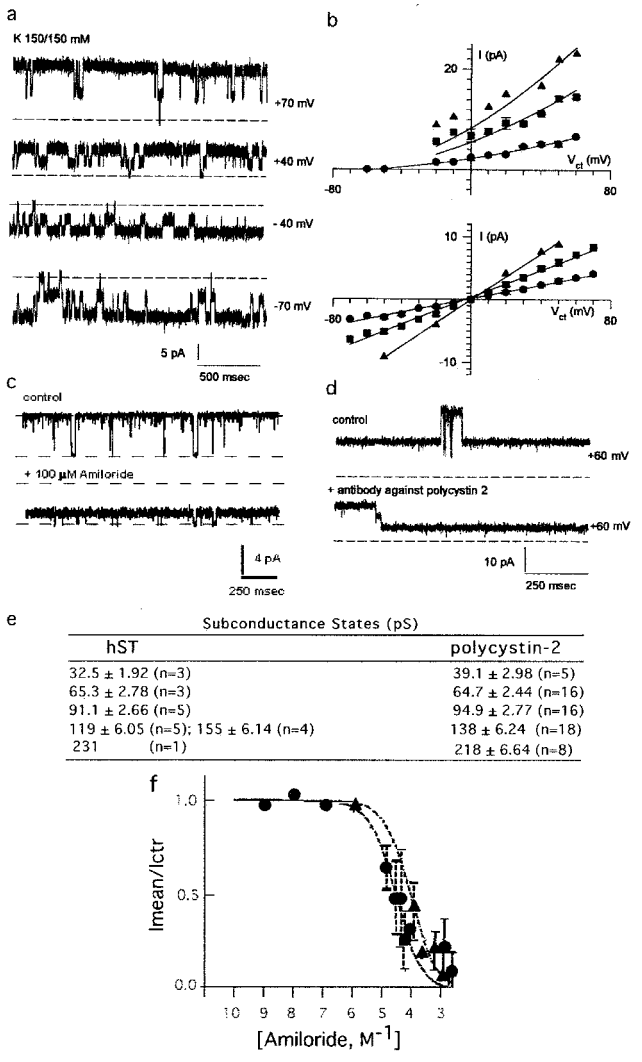

Fig. 4. Recombinant polycystin-2 is a nonselective cation channel. (*a*) Single K^+ currents of flag-tagged purified polycystin-2 obtained in symmetrical K^+. (*b*) Current-to-voltage relationships in asymmetrical K^+ (*Upper*, $n = 5$), and symmetrical K^+ (*Lower*, $n = 5$). (*c*) Polycystin-2 K^+ channel activity was inhibited by amiloride ($n = 18$). (*d*) Polycystin-2-mediated single K^+ currents were inhibited by anti-polycystin-2 antibody (1:10 dilution, $n = 3$). (*e*) Comparison of most frequent single channel conductance substates in hST and flag-tagged polycystin-2. (*f*) Dose-response of amiloride. The effect of increasing concentrations of amiloride on the known single-current for hST (filled circles, $n = 10$), and Sf9 purified material, $n = 5$, as fitted to the equation $1 - ([Amil]/[Amil] + K_i)$, where [Amil] = molar concentration of amiloride, obtaining a K_i of 27.0 and 79.4 μM, respectively.

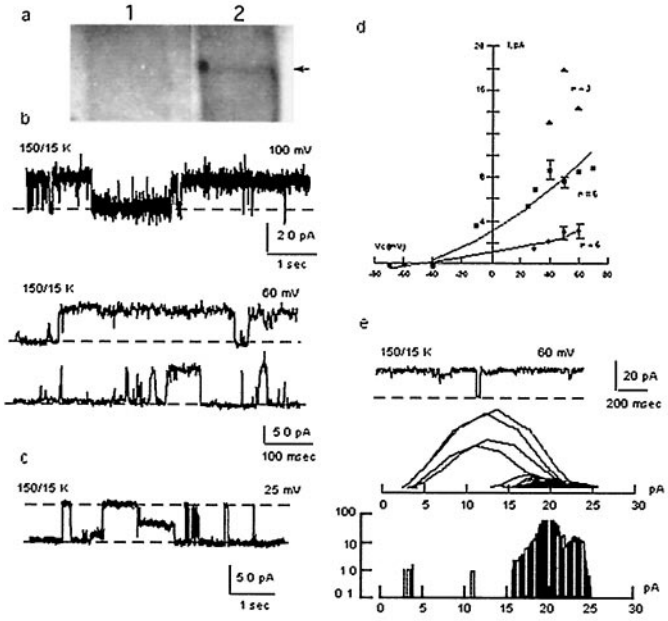

Fig. 5. Cation selective channel activity of *in vitro* translated polycystin-2. (*a*) *In vitro* translated S^{35}-labeled polycystin-2 identified by autoradiography after SDS/PAGE. Lane 1, control in the absence of *PKD2*-containing plasmid. Lane 2, polycystin-2 (110 kDa). Luciferase, with an expected 61 kDa was used as positive control (data not shown). (*b*) Single channel currents of *in vitro* translated polycystin-2 in a chemical K^+ gradient ($n = 24$). Different conductance states are shown (*Top* and *Middle*). (*c*) Conductance substates are also observed in single channel tracings ($n = 3$). (*d*) Current-to-voltage relationships in asymmetrical K^+. Single channel conductance substates are shown. (*e*) Small subconductance states can be observed in large conductance openings by mean vs. variance analysis as in Fig. 1c.

the homolog polycystin-L (17). These included a large single conductance, permeability to the monovalent cations K^+ and Na^+, permeability to Ca^{2+}, and inhibition by Ca^{2+}, La^{3+}, and Gd^{3+}, and by a reduction in pH (in this case, only the open channel probability, but not the single channel conductance was affected). These features distinguish polycystin-2 from TRP channels and voltage-gated Ca^{2+} channels, with which it also shares sequence homology (6, 18). Polycystin-2 channel activity was highly similar among the three preparations tested (hST, Sf9 *PKD2* baculovirus-infected cells, and *in vitro* translation product). Among the similarities are the main single channel conductance, the multiple subconductance states, the permeability to divalent cations, and inhibition by Gd^{3+} and La^{3+}, and pH. The *in vitro* translated material showed strong voltage dependence. However, it remains possible that intracellular proteins in the hST and Sf9 materials, may also play a regulatory role in polycystin-2 voltage dependence. Further, polycystin-2, from all three preparations (hST, insect cells, and *in vitro* translation) was inhibited by amiloride, reflecting functional similarities with other cation-selective epithelial ion channels (14–16). The effect of amiloride may also explain previous findings indicating its inhibitory effect on cation transport in human placenta (22). Amiloride-sensitive cation transport has also been observed in ADPKD renal cysts (23). Interestingly, the presence of multiple conductance substates in all three preparations may imply various states of protein oligomerization, which may be implicated in simultaneous gating. Hetero-oligomerization of polycystin-2 with other proteins, including polycystin-1, has been described (10, 24, 25) and may perhaps serve a regulatory function (7).

It is intriguing that, despite structural homology, ubiquitous tissue distribution (10, 13, 18, 26), and similar channel properties (17, this report), defects only in polycystin-2 but not polycystin-L cause ADPKD. Two possibilities could be considered in this regard. First, in the original report (17), polycystin-L mRNA was microinjected into oocytes, and patch-clamping of the plasma membrane revealed a channel with features similar to those described here for polycystin-2. It may be argued that overexpression of polycystin-L in oocytes may cause the translocation of an endogenous pool of polycystin-2 to the surface membrane where it can be detected functionally. Evaluation of the functional status of *in vitro* translated polycystin-L will be required to exclude this possibility. A second possibility is that, despite similar tissue expression, the cellular and subcellular distribution of polycystin-2 and polycystin-L may be different [e.g., we could

not detect polycystin-L in hST, despite its reported presence in human placenta (13)]. Alignment of the two proteins reveals that polycystin-2 contains a C-terminal cytoplasmic domain lacking in polycystin-L (13). Thus each channel protein may be involved in distinct signaling pathways, aberrations of which may lead to nonoverlapping disease phenotypes.

ADPKD is associated with fluid-filled cysts where altered electrolyte transport, including Na^+, Cl^-, and possibly Ca^{2+}, has been implicated in the onset of the disease (2, 8). The channel properties of polycystin-2 may now help explain some of these functional features. Polycystin-2 can function as a distinct channel in the absence of associated proteins. Mutations in polycystin-2 found in ≈10–15% of patients with ADPKD may directly impair normal ion transport in affected cells, thus leading to cyst formation. Further, polycystin-1, the protein mutated in ≈85% of cases of ADPKD, has been shown to directly interact with polycystin-2, at least *in vitro* (24, 25). It is therefore likely that mutations in polycystin-1 may also impair normal channel activity of polycystin-2. Additional experiments will be needed to validate these hypotheses. Finally, the presence of a novel nonselective cation channel in full-term hST may contribute to the maintenance of fetal electrolytic homeostasis, and in particular, the apical placental transfer of cations between mother and fetus.

We thank Dr. Stephan Somlo for his kind gift of the partial *PKD2* cDNA clone K1-1, and Ms. Monica Zaucha, G. Robert Jackson, Jr. and Dr. Alan S. Lader for excellent technical support. The studies were supported by National Institutes of Health Grant P01 DK54711 (to M.A.A. and K.K.), and by Universidad de Buenos Aires Secretaría de Ciencia y Técnica (UBACyT) TB65, Consejo Nacional de Investigaciones Científicas y Técnicas de Argentina (CONICET) PIP 4549/96, and Agencia Nacional de Promoción Científica y Tecnológica (ANPCyT), Proyecto de Investigación Científica y Tecnológica (PICT) 1594 (to C.I., I.R., A.D., and E.Z.).

1. Dalgaard, O. Z. (1957) *Acta Med. Scand. Suppl.* **328,** 1–255.
2. Arnaout, M. A. (2001) *Annu. Rev. Med.* **52,** 93–123.
3. Grantham, J. J. (1993) *J. Am. Soc. Nephrol.* **3,** 1843–1857.
4. The European Polycystic Kidney Disease Consortium (1994) *Cell* **77,** 881–894.
5. The International Polycystic Kidney Disease Consortium (1995) *Cell* **81,** 289–298.
6. Mochizuki, T., Wu, G., Hayashi, T., Xenophontos, S. L., Veldhuisen, B., Saris, J. J., Reynolds, D. M., Cai, Y., Gabow, P. A., Pierides, A., *et al*. (1996) *Science* **272,** 1339–1342.
7. Emmons, S. W. & Somlo, S. (1999) *Nature (London)* **401,** 339–340.
8. Sullivan, L. P., Wallace, D. P. & Grantham, J. J. (1998) *Physiol. Rev.* **78,** 1165–1191.
9. Stulc, J. (1997) *Physiol. Rev.* **77,** 805–836.
10. Ong, A. C., Ward, C. J., Butler, R. J., Biddolph, S., Bowker, C., Torra, R., Pei, Y. & Harris, P. C. (1999) *Am. J. Pathol.* **154,** 1721–1729.
11. Grosman, C., Mariano, M. I., Bozzini, J. P. & Reisin, I. L. (1997) *J. Membr. Biol.* **157,** 83–95.
12. Hille, B. (1992) *Ionic Channels of Excitable Membranes* (Sinauer, Sunderland, MA).
13. Nomura, H., Turco, A. E., Pei, Y., Kalaydjieva, L., Schiavello, T., Weremowicz, S., Ji, W., Morton, C. C., Meisler, M., Reeders, S. T. & Zhou, J. (1998) *J. Biol. Chem.* **273,** 25967–25973.
14. Light, D. B., McCann, F. V., Keller, T. M. & Stanton, B. A. (1988) *Am. J. Physiol.* **255,** F278–F286.
15. Cantiello, H. F., Stow, J., Prat, A. G. & Ausiello, D. A. (1991) *Am. J. Physiol.* **261,** C882–C888.
16. Canessa, C., Horisberger, J.-D. & Rossier, B. (1993) *Nature (London)* **361,** 467–470.
17. Chen, X. Z., Vassilev, P. M., Basora, N., Peng, J. B., Nomura, H., Segal, Y., Brown, E. M., Reeders, S. T., Hediger, M. A. & Zhou, J. (1999) *Nature (London)* **401,** 383–386.
18. Cai, Y., Maeda, Y., Cedzich, A., Torres, V. E., Wu, G., Hayashi, T., Mochizuki, T., Park, J. H., Witzgall, R. & Somlo, S. (1999) *J. Biol. Chem.* **274,** 28557–28565.
19. Bosch, I., Jackson, G., Croop, J. & Cantiello, H. (1996) *Am. J. Physiol.* **271,** C1527–C1538.
20. Kunze, D. L., Sinkins, W. G., Vaca, L. & Schilling, W. P. (1997) *Am. J. Physiol.* **272,** C27–C34.
21. Hviid Larsen, E., Gabriel, S. E., Stutts, M. J., Fullton, J., Price, E. M. & Boucher, R. C. (1996) *J. Gen. Physiol.* **107,** 695–714.
22. Faller, D., O'Reilly, C. & Ryan, M. (1994) *Biochem. Pharmacol.* **47,** 757–761.
23. Perrone, R. D. (1985) *J. Clin. Invest.* **76,** 1688–1691.
24. Qian, F., Germino, F. J., Cai, Y., Zhang, X., Somlo, S. & Germino, G. G. (1997) *Nat. Genet.* **16,** 179–183.
25. Tsiokas, L., Kim, E., Arnould, T., Sukhatme, Y. P. & Walz, G. (1997) *Proc. Natl. Acad. Sci. USA* **94,** 6965–6970.
26. Foggensteiner, L., Bevan, A. P., Thomas, R., Coleman, N., Boulter, C., Bradley, J., Ibraghimov-Beskrovnaya, O., Klinger, K. & Sandford, R. (2000) *J. Am. Soc. Nephrol.* **11,** 814–827.